

1 **Variability and Uncertainty in Flux-Site Scale Net Ecosystem**
2 **Exchange Simulations Based on Machine Learning and**
3 **Remote Sensing: A Systematic Evaluation**

4 Haiyang Shi^{1,2,4,5}, Geping Luo^{1,2,3,5}, Olaf Hellwich⁶, Mingjuan Xie^{1,2,4,5}, Chen Zhang^{1,2}, Yu Zhang^{1,2}, Yuangang
5 Wang^{1,2}, Xiuliang Yuan¹, Xiaofei Ma¹, Wenqiang Zhang^{1,2,4,5}, Alishir Kurban^{1,2,3,5}, Philippe De Maeyer^{1,2,4,5} and
6 Tim Van de Voorde^{4,5}

7
8 ¹ State Key Laboratory of Desert and Oasis Ecology, Xinjiang Institute of Ecology and Geography, Chinese
9 Academy of Sciences, Urumqi, Xinjiang, 830011, China.

10 ² University of Chinese Academy of Sciences, 19 (A) Yuquan Road, Beijing, 100049, China.

11 ³ Research Centre for Ecology and Environment of Central Asia, Chinese Academy of Sciences, Urumqi, China.

12 ⁴ Department of Geography, Ghent University, Ghent 9000, Belgium.

13 ⁵ Sino-Belgian Joint Laboratory of Geo-Information, Ghent, Belgium and Urumqi, China.

14 ⁶ Department of Computer Vision & Remote Sensing, Technische Universität Berlin, 10587 Berlin, Germany.

15

16 **Correspondence to:** Geping Luo (luogp@ms.xjb.ac.cn) and Olaf Hellwich (olaf.hellwich@tu-berlin.de)

17 Submitted to *Biogeosciences*

18 **Abstract.** Net ecosystem exchange (NEE) is an important indicator of carbon cycling in terrestrial ecosystems.
19 Many previous studies have combined flux observations, meteorological, biophysical, and ancillary predictors
20 using machine learning to simulate the site-scale NEE. However, systematic evaluation of the performance of
21 such models is limited. Therefore, we performed a meta-analysis of these NEE simulations. A total of 40 such
22 studies and 178 model records were included. The impacts of various features throughout the modeling process
23 on the accuracy of the model were evaluated. Random Forests and Support Vector Machines performed better
24 than other algorithms. Models with larger time scales have lower average R-squared, especially when the time
25 scale exceeds the monthly scale. Half-hourly models (average R-squared = 0.73) were significantly more
26 accurate than daily models (average R-squared = 0.5). There are significant differences in the predictors used
27 and their impacts on model accuracy for different plant functional types (PFTs). Studies at continental and
28 global scales (average R-squared = 0.37) with multiple PFTs, more sites, and a large span of years correspond to
29 lower R-squared than studies at local (average R-squared = 0.69) and regional scales (average R-squared = 0.7).
30 Also, the site-scale NEE predictions need more focus on the internal heterogeneity of the NEE dataset and the
31 matching of the training set and validation set.

32 **1 Introduction**

33 Net ecosystem exchange (NEE) of CO₂ is an important indicator of carbon cycling in terrestrial ecosystems (Fu
34 et al., 2019), and accurate estimation of NEE is important for the development of global carbon neutral policies.
35 Although process-based models have been used for NEE simulations (Mitchell et al., 2009), their accuracy and
36 spatial resolutions of the model outputs are limited probably due to the lack of understanding and quantification
37 of complex processes. Many researchers have tried to use a data-driven approach as an alternative (Fu et al.,
38 2014; Tian et al., 2017; Tramontana et al., 2016; Jung et al., 2011). On the one hand, it was made possible by
39 the increase in the growth of global carbon flux observations and the large amount of flux observation data
40 being accumulated. Since the 1990s, the use of the eddy covariance technique to monitor NEE has been rapidly
41 promoted (Baldocchi, 2003). Several regional and global flux measurement networks have been established for
42 the big data management of the flux sites, including CarboEuro-flux (Europe), AmeriFlux (North America),
43 OzFlux (Australia), ChinaFlux (China), FLUXNET (global), etc. On the other hand, machine learning
44 approaches are increasingly used to extract patterns and insights from the ever-increasing stream of geospatial
45 data (Reichstein et al., 2019). The rapid development of various algorithms and high public availability of model
46 tools in the field of machine learning have made these techniques easily available to more researchers in the
47 field of geography and ecology (Reichstein et al., 2019). Since the above two major advances (i.e., increasing
48 availability of flux data and machine learning techniques) in the last two decades, various machine learning
49 algorithms have been used to simulate NEE at the flux station scale with various predictor variables (e.g.,
50 meteorological variables, biophysical variables) incorporated for spatial and temporal mapping of NEE or
51 understanding the driving mechanisms of NEE.

52
53 To date, studies on using machine learning to predict NEE have a high diversity in terms of modeling
54 approaches. To obtain a comprehensive understanding of machine learning-based NEE prediction, a synthesis
55 evaluation of these machine learning models is necessary. Since the beginning of this century, when machine

56 learning approaches were still rarely used in geography and ecology research, neural networks were already
57 used to perform simulations and mapping of NEE in European forests (Papale and Valentini, 2003).
58 Subsequently, considerable efforts have been made by researchers to improve such predictive models. Many
59 studies have demonstrated the effectiveness of their proposed improvements (i.e., using predictors with a higher
60 spatial resolution (Reitz et al., 2021) and using data from the local flux site network (Cho et al., 2021)) by
61 comparing with previous studies. However, the improvements achieved in these studies may be limited to
62 smaller areas and specific conditions and may not be generalizable (Cleverly et al., 2020; Reed et al., 2021; Cho
63 et al., 2021). We are more interested in guidelines with universal applicability that improve the model accuracy,
64 such as the selection of appropriate predictors and algorithms under different conditions. Therefore, we should
65 synthesize the results of models applied to different conditions and regions to obtain general insights.

66

67 Many factors may affect the performance of these NEE prediction models, such as the predictor variables, the
68 spatial and temporal span of the observed flux data, the plant functional type (PFT) of the flux sites, the model
69 validation method, the machine learning algorithm used, as described below:

70 a) Predictors: Various biophysical variables (Zeng et al., 2020; Cui et al., 2021; Huemmrich et al., 2019) and
71 other meteorological and environmental factors have been used in the simulation of NEE. The most
72 commonly used predictor variables include precipitation (Prec), air temperature (Ta), wind speed (Ws),
73 net/sun radiation (Rn/Rs), soil temperature (Ts), soil texture, soil moisture (SM) (Zhou et al., 2020), vapor-
74 pressure deficit (VPD) (Moffat et al., 2010; Park et al., 2018), the fraction of absorbed photosynthetically
75 active radiation (FAPAR) (Park et al., 2018; Tian et al., 2017), vegetation index (e.g., NDVI, EVI), LAI,
76 and evapotranspiration (ET) (Berryman et al., 2018). The predictor variables used vary with the natural
77 conditions and vegetation functional types of the study area. In contrast, in models that include multiple
78 PFTs, some variables that play a significant role in the prediction of each of the multiple PFTs may have
79 higher importance. For example, growing degree days (GDD) may be a more effective variable for NEE of
80 tundra in the northern hemisphere high latitudes (Virkkala et al., 2021), while measured groundwater levels
81 may be important for wetlands (Zhang et al., 2021). Some of these predictor variables are measured at flux
82 stations (e.g., meteorological factors such as precipitation and temperature), while others are extracted
83 from reanalyzed meteorological datasets and satellite remote sensing image data (e.g., vegetation indices).
84 The spatial and temporal resolution of predictors can lead to differences in their relevance to NEE
85 observations. Most measured in situ meteorological factors have a good spatio-temporal match to the
86 observed NEE (site scale, half-hourly scale). However, the proportion of NEE explained by remotely
87 sensed biophysical covariates may depend on their spatial and time scales. For example, the MODIS-based
88 8-daily NDVI data may better capture temporal variation in the relationship between NEE and vegetation
89 growth than the Landsat-based 16-daily NDVI data. In contrast, the interpretation of NEE by variables
90 such as soil texture and soil organic content (SOC), which do not have temporal dynamic information, may
91 be limited to the interpretation of spatial variability, although they are considered to be important drivers of
92 NEE. Therefore, the importance of variables obtained from NEE simulations based on a data-driven
93 approach may differ from that in process-based models as well as in the actual driving mechanisms. This
94 may be related to the spatial and temporal resolution of the predictors used and the quality of the data. It is

95 necessary to consider the spatio-temporal resolution of the data for the actual biophysical variables used in
96 the different studies in the systematic evaluation of data-driven NEE simulations.

- 97 b) The spatio-temporal heterogeneity of data sets, and validation method: The spatio-temporal heterogeneity
98 of the dataset may affect model accuracy. Typically, training data with larger regions, multiple sites,
99 multiple PFTs, and longer spans of years may have a higher degree of imbalance (Kaur et al., 2019; Van
100 Hulse et al., 2007; Virkkala et al., 2021; Zeng et al., 2020). Modeling with unbalanced data (where the
101 difference between the distribution of the training and validation sets is significant even if selected at
102 random) may result in lower model accuracy. To date, the most commonly used methods for validating
103 such models include spatial (Virkkala et al., 2021), temporal (Reed et al., 2021), and random (Cui et al.,
104 2021) cross-validation. The imbalance of data between the training and validation sets may affect the
105 accuracy of the models when using these validation methods. Spatial validation is used to assess the ability
106 of the model to adapt to different regions or flux sites of different PFTs, and a common method is 'leave
107 one site out' cross-validation (Virkkala et al., 2021; Zeng et al., 2020). If the data from the site left out is
108 not covered (or partially covered) by the distribution of the training dataset, the model's prediction
109 performance at that site may be poor due to the absence of a similar type in the training set. Temporal
110 validation typically uses some years of data as training and the remaining years as validation to assess the
111 model's fitness for interannual variability. For a year that is left out (e.g. a special extreme drought year
112 which does not occur in the training set), the accuracy of the model may be limited if there are no similar
113 years (extreme drought years) in the training dataset. K-fold cross-validation is commonly used in random
114 cross-validation to assess the fitness of the model to the spatio-temporal variability. In this case, different
115 values of K may also have a significant impact on the model accuracy. For example, for an unbalanced
116 dataset, the average model accuracy obtained from a 10-fold ($K = 10$) validation approach is likely to be
117 higher than that of a 3-fold ($K = 3$) validation approach (Marcot and Hanea, 2021).
- 118 c) Machine learning algorithms used: Simulating NEE using different machine learning algorithms may
119 influence the model accuracy, which may be induced by the characteristics of these algorithms themselves
120 and the specific data distribution of the NEE training set. For example, Neural Networks can be used
121 effectively to deal with nonlinearities, while as an ensemble learning method, Random Forests can avoid
122 overfitting due to the introduction of randomness. Therefore, a comprehensive evaluation of this is
123 necessary.

124
125 In this study, to evaluate the impacts of predictors use, algorithms, spatial/time scale, and validation methods on
126 model accuracy, we performed a meta-analysis of papers with prediction models that combine NEE
127 observations from flux towers, various predictors, and machine learning for the data-driven NEE simulations. In
128 addition, we also analyzed the causality of multiple features in NEE simulations and the joint effects of multiple
129 features on model accuracy using the Bayesian Network (BN) (a multivariate statistical analysis approach
130 (Pearl, 1985)). The findings of this study can provide some general guidance for future NEE simulations.

131 **2 Methodology**

132 **2.1 Criteria for including articles**

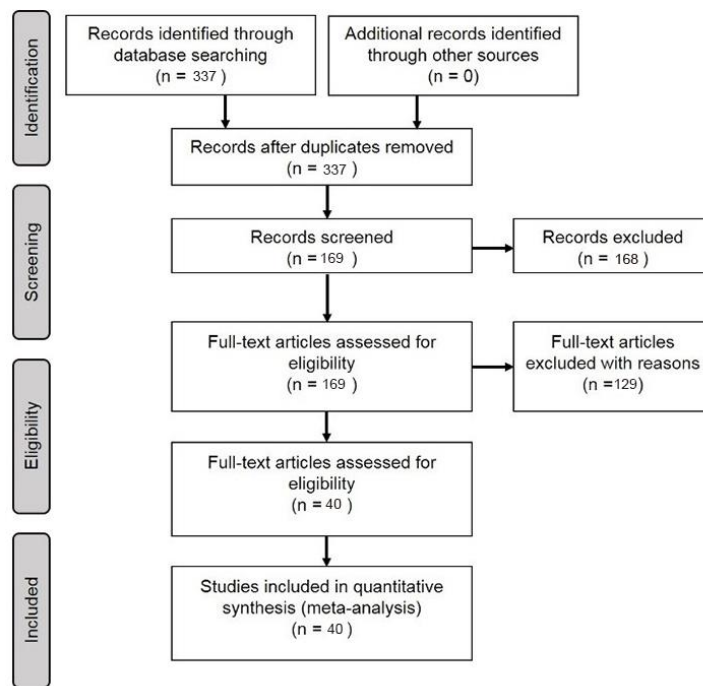
133 In the Scopus database, a literature query was applied to titles, abstracts, and keywords (Table 1) according to
134 Preferred Reporting Items for Systematic Reviews and Meta-Analyses (PRISMA) (Moher et al., 2009) (Fig. 1):

- 135 a) Articles were filtered for those that modeled NEE. Articles that modeled other carbon fluxes such as
136 methane flux were not included.
- 137 b) Articles that used only univariate regression rather than multiple regression were screened out.
- 138 c) Articles reported the determination coefficient (R-squared) of the validation step (Shi et al., 2021;
139 Tramontana et al., 2016; Zeng et al., 2020) as the measure of model performance. Although RMSE is also
140 often used for model accuracy assessment, its dependence on the magnitude of water flux values makes it
141 difficult to use for fair comparisons between studies.
- 142 d) Articles were published in journals with language limited to English.
- 143 e) Articles were filtered for those that were published in the specific journals (Table S1) for research quality
144 control because the data, model implements, and peer review in these journals are often more reliable.

145
146 Table 1. Article search query design: '[A1 OR A2 OR A3...] AND [B1 OR B2...] AND [C1 OR C2...]'

ID	A	B	C
1	Carbon flux	"Eddy covariance"	"machine learning"
2	CO ₂ flux	"Flux tower"	regress*
3	"net ecosystem exchange"		"Support Vector"
4	net ecosystem produc		"Neural Network"
5	gross primary produc		"Random Forest"
6	Carbon exchange		

147



148

149 Figure 1. PRISMA-based paper filtering flowchart.

150 **2.2 Features of prediction models**

151 Typically, the flow of the NEE prediction modeling framework (Fig. 2) based on flux observations and machine
 152 learning is as follows: first, half-hourly scale NEE flux observations are aggregated into various time scale NEE
 153 data, and gap-filling techniques (Moffat et al., 2007) are often used in this step to obtain complete NEE series
 154 when data are missing. Various predictors including meteorological variables, remote sensing-based biophysical
 155 variables, etc. are extracted to match site-scale NEE series to generate a training dataset containing the target
 156 variable NEE and various covariates. Subsequently, various algorithms are used for the NEE prediction model
 157 construction and validated in different ways (e.g., leave-one-site-out validation (Zeng et al., 2020)). Finally, in
 158 some studies, prediction models were applied on gridded covariate data to map the regional or global-scale NEE
 159 spatial and temporal variations (Zeng et al., 2020; Papale and Valentini, 2003; Jung et al., 2020). The
 160 information of R-squared (at the validation phase) and the associated model features reported in the article are
 161 considered as one data record for the formal meta-analysis (i.e., each R-squared record corresponding to a
 162 prediction model). From the included papers, R-squared records and various features (Table 2) involved in the
 163 NEE modeling framework (Fig. 2) were extracted (including the used algorithms, modeling/validation methods,
 164 remote sensing data, meteorological data, biophysical data, and ancillary data). In some studies, multiple
 165 algorithms were applied to the same dataset, or models with different features were developed (Virkkala et al.,
 166 2021; Zhang et al., 2021; Cleverly et al., 2020; Tramontana et al., 2016). In these cases, multiple data records
 167 will be documented.

168

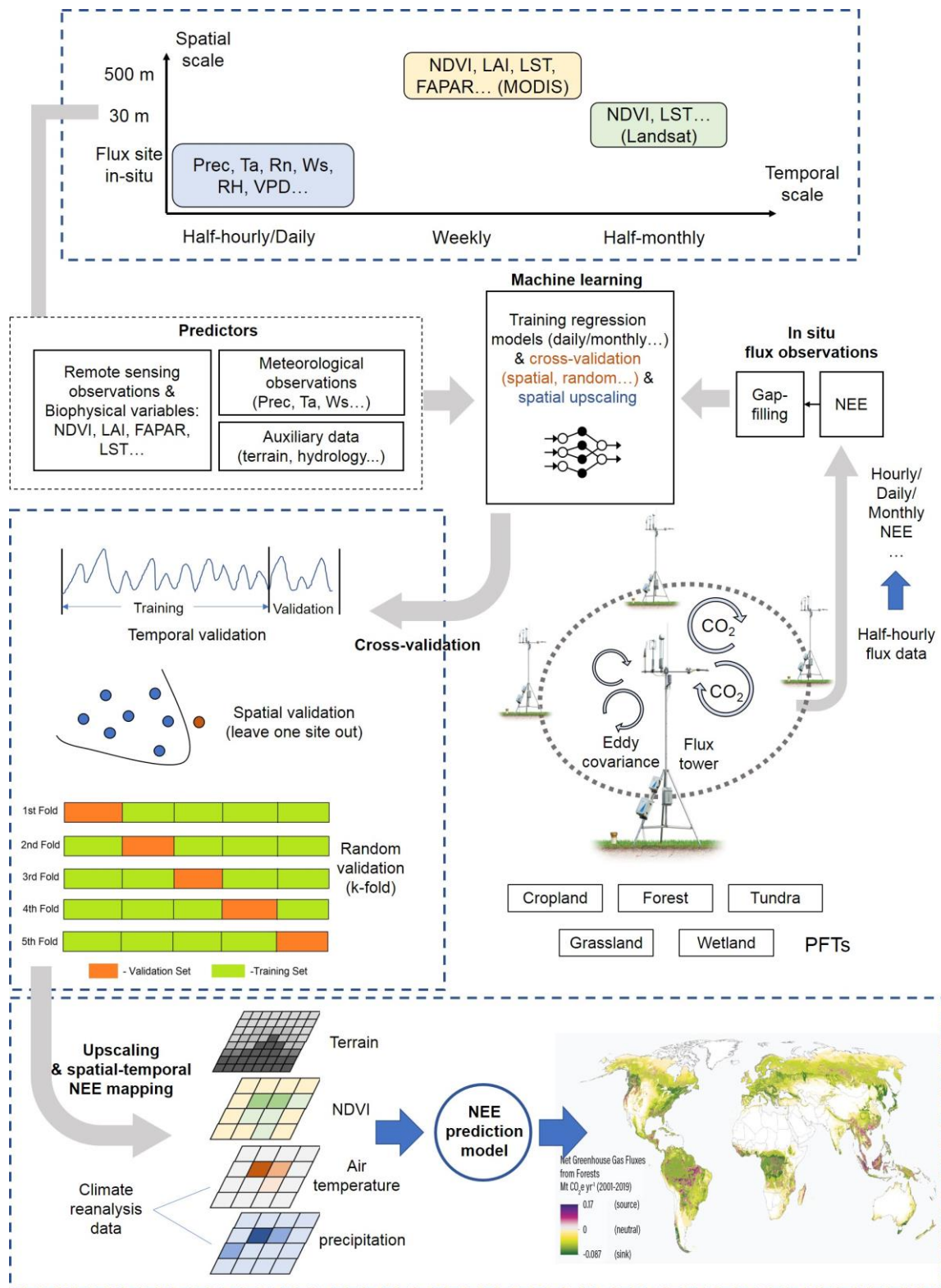
169 In the practical information extracting step, we categorized such features in a comparable manner. First, we
 170 categorized the various algorithms used in these papers, although the same algorithm may also have a variant

171 form or an optimized parameter scheme. They are categorized into the following families of algorithms:
172 Random Forests (RF), Multiple Linear Regressions (MLR), Artificial Neural Networks (ANN), Support Vector
173 Machines (SVM), Partial Least Squares Regression (PLSR), Generalized additive model (GAM), Boosted
174 Regression Tree (BRT), Bayesian Additive Regression Trees (BART), Cubist, model tree ensembles (MTE).
175 Second, we classified the spatial scales of these studies. Models with study areas (spatial extent covered by flux
176 stations) smaller than 100x100 km were classified as ‘local’ scale models, those with study area sizes exceeding
177 continental scale were classified as ‘global’ scale, and those with study area sizes in between were classified as
178 ‘regional’ scale. Third, for various predictors, we only recorded whether the predictors were used or not without
179 distinguishing the detailed data sources and categories (e.g., grid meteorological data from various reanalysis
180 datasets and in-situ meteorological observations from flux stations), measurement methods (e.g., soil moisture
181 measured/estimated by remote sensing or in situ sensors), etc. Fourth, we documented PFTs for the prediction
182 models from the description of study areas or sites in these papers. They are classified into the following types:
183 forest, grassland, cropland, wetland, savannah, tundra, and multi-PFTs (models containing a mixture of multiple
184 PFTs). Models not belonging to the above PFTs were not given a PFT field and were not included in the
185 subsequent analysis of the PFT differences. Other features (Table 2) are extracted directly from the
186 corresponding descriptions in the papers in an explicit manner.

187

188 Subsequently, the model accuracies corresponding to different levels of various features are compared in a
189 cross-study fashion. In the evaluation of algorithms and time scales, we also implement comparisons within
190 individual studies. For example, in the evaluation of the effects of the algorithms, we compare the accuracy of
191 models using the same training data and keeping other features as constants in individual studies. In this intra-
192 study comparison step, only algorithms with relatively large sample sizes in the cross-study comparisons were
193 selected.

194



195

196

197

198

199

200

201

Figure 2. Features of the machine learning-based NEE prediction process. The flux tower photo is from <https://www.licor.com/env/support/Eddy-Covariance/videos/ec-method-02.html> (last accessed: 23rd March 2022). The map in the lower part is from Harris et al., 2021. Prec, Ta, Rn, Ws, RH, and VPD represent precipitation, air temperature, net surface radiation, wind speed, relative humidity, and vapour-pressure deficit respectively. FAPAR is the fraction of absorbed photosynthetically active radiation. LST is the land surface temperature. LAI is the leaf area index.

203 Table 2. Description of information extracted from the included papers.

Field/Feature	Definition	Categories adopted
Id paper	Identification number of the paper (internal)	
Paper	Paper metadata	
Author/s	Name/s of author/s	
Title	Title of the paper	
Year	Year of publication	
Publication title	Name of the journal where the paper was published	
Plant functional type (PFT)	PFTs for the flux sites used	1-forest, 2-grassland, 3-cropland, 4-wetland, 5-savannah, 6-tundra and multi-PFTs
Location	More precise location (with the latitude and longitude of the center of the studied sites). Global (mainly based on FluxNet (Tramontana et al., 2016)) and continental-scale studies are not shown on the map due to the difficulty of identifying specific locations.	latitude, longitude
Algorithms	Algorithm families used in the multivariate regression	Random Forests (RF), Multiple Linear Regressions (MLR), Artificial Neural Networks (ANN), Support Vector Machines (SVM), Partial Least Squares Regression (PLSR), Generalized additive model (GAM), Boosted Regression Tree (BRT), Bayesian Additive Regression Trees (BART), Cubist, model tree ensembles (MTE).
Sites number	Number of the flux sites used	
Study area/Spatial scale	Area representatively covered by the flux sites	local (less than 100×100 km), regional, global (continent-scale and global scale)
Time scale	The time scale of the model	half-hourly, hourly, daily, weekly, 8-daily, monthly, seasonally, yearly
Study period	The period of the data used in the model	year, growing season, daytime, spring, summer, autumn, winter
Year span	The span of years of the flux data used	
Site year	Describe the volume of total flux data with the number of sites and years aggregated.	
Cross-validation	Describe the chosen method of cross-validation.	Spatial (e.g., 'leave one site out'), temporal (e.g., 'leave one year out'), random (e.g., 'k-fold')

Training/validation	Describe the ratio of the data in training and validation sets.	
Satellite images	Describe the source of satellite images used to derive NDVI, EVI, LAI, LST, etc.	Landsat, MODIS, Hyperion (EO-1), AVHRR, IKONOS
Biophysical predictors	LAI, NDVI/EVI, evapotranspiration (ET) (i.e., the latent heat observed by the flux station), enhanced vegetation index (EVI), the fraction of absorbed photosynthetically active radiation/photosynthetically active radiation (FAPAR/PAR), leaf area index (LAI), etc.	Used (recorded as '1') or not used (recorded as '0')
Meteorological variables	precipitation (Prec), net radiation/solar radiation (Rn/Rs), air temperature (Ta), vapour-pressure deficit (VPD), relative humidity (RH) , etc.	Used (recorded as '1') or not used (recorded as '0')
Ancillary data	Describe the source of ancillary variables including terrain variables derived from DEM, soil texture, or hydrology-related data: soil organic content (SOC), soil texture, terrain, soil moisture/land surface water index (SM_LSWI), etc.	Used (recorded as '1') or not used (recorded as '0')
Top three variables in the ranking of importance of predictors	Describe the interpretation of the importance of variables in machine learning models.	
Accuracy measure	Accuracy measure used to assess the performance of the estimation/prediction	R-squared (in the validation phase)

204

205 2.3 Bayesian Network for analyzing joint effects

206 Based on the Bayesian network (BN), the joint impacts of multiple model features on the R-squared are
207 analyzed. A BN can be represented by nodes (X_1, \dots, X_n) and the joint distribution (Pearl, 1985):

$$208 \quad P(X) = P(X_1, X_2, \dots, X_n) = \prod_{i=1}^n P(X_i | pa(X_i)) \quad (1)$$

209 where $pa(X_i)$ is the probability of the parent node X_i . Expectation-maximization (EM) approach (Moon, 1996) is
210 used to incorporate the collected model records and compile the BN.

211

212 Sensitivity analysis is used for the evaluation of node influence based on mutual information (MI) which is
213 calculated as the entropy reduction of the child node resulting from changes at the parent node (Shi et al., 2020):

214
$$MI = H(Q) - H(Q|F) = \sum_q \sum_f P(q, f) \log_2 \left(\frac{P(q, f)}{P(q)P(f)} \right) \quad (2)$$

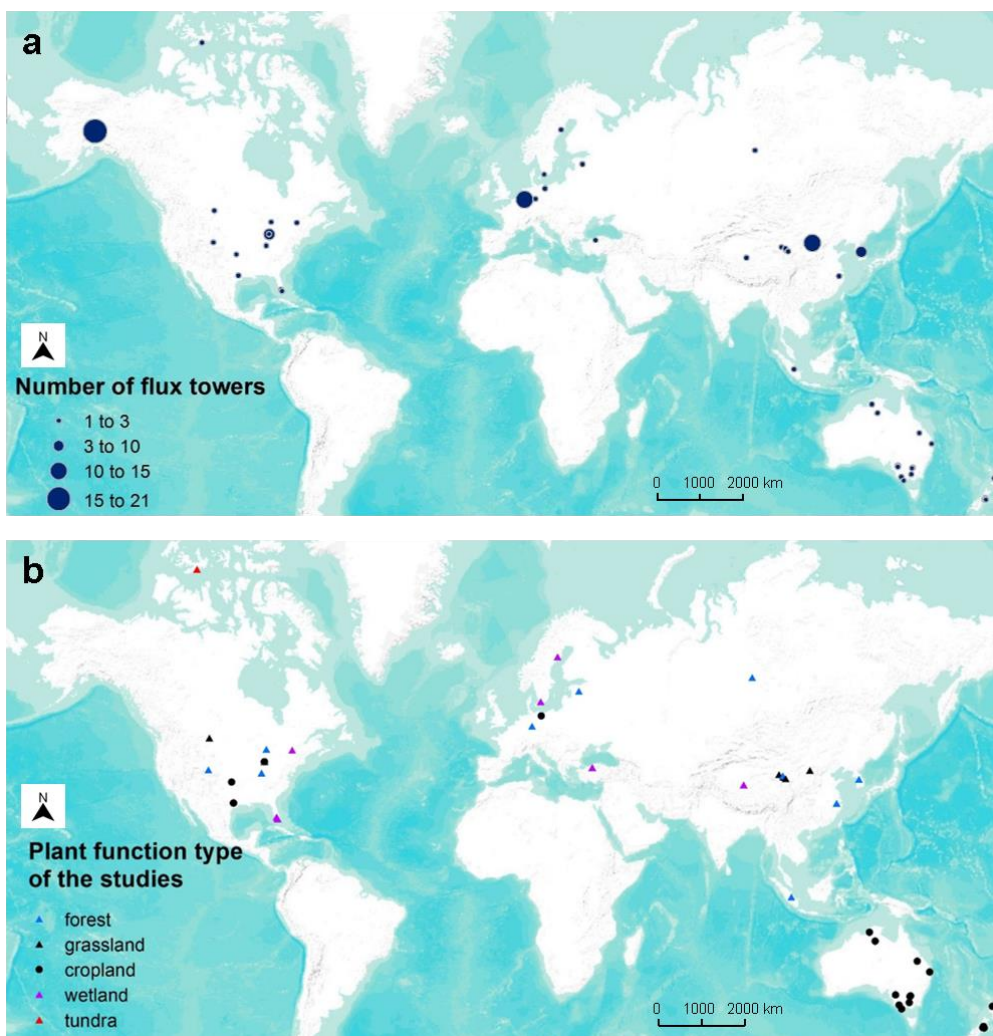
215 where H represents the entropy, Q represents the target node, F represents the set of other nodes and q and f
 216 represent the status of Q and F.

217 **3 Results**

218 **3.1 Articles included in the meta-analysis**

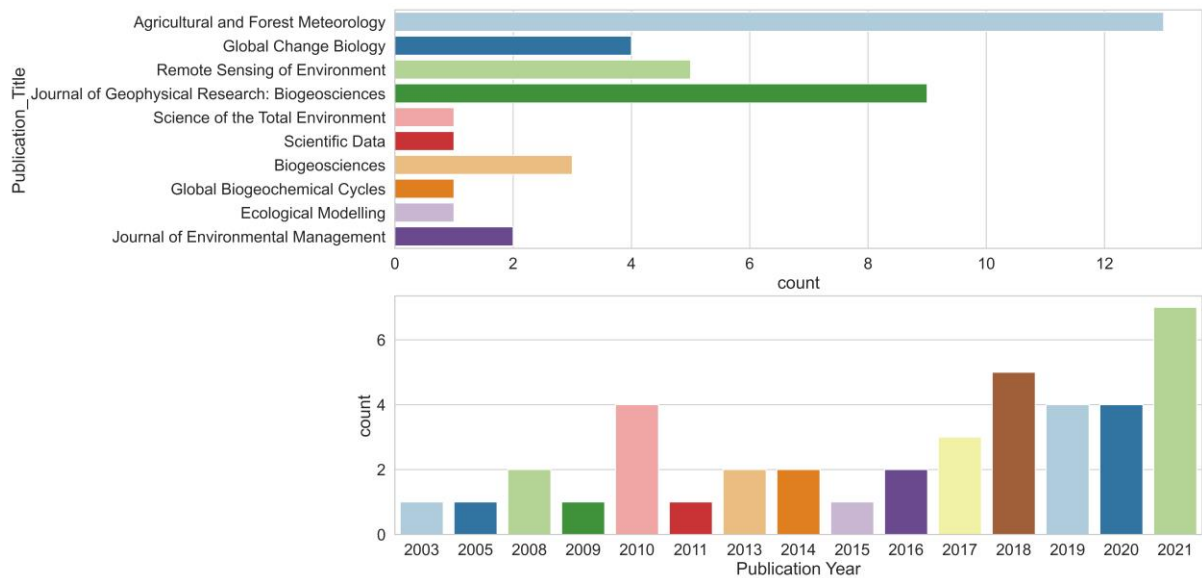
219 We included 40 articles (Table S2) and extracted 178 model records for the formal meta-analysis (Fig. 1). Most
 220 studies were implemented in Europe, North America, Oceania, and China (Fig. 3). The number of such papers is
 221 increasing recently (Fig. 4) and it shows the machine learning approach for NEE prediction has been of interest
 222 to more researchers. The main journals in which these articles have been published (Fig. 4) include Remote
 223 Sensing of Environment, Global Change Biology, Agricultural and Forest Meteorology, Biogeosciences, and
 224 Journal of Geophysical Research: Biogeosciences, etc.

225



226
 227 Figure 3. Location of studies (a) included with the number of flux sites included and (b) their PFTs in the meta-
 228 analysis (total of 40 studies and 178 model records). Global (mainly based on FluxNet (Tramontana et al.,

229 2016)) and continental-scale studies are not shown on the map due to the difficulty of identifying specific
 230 locations.
 231



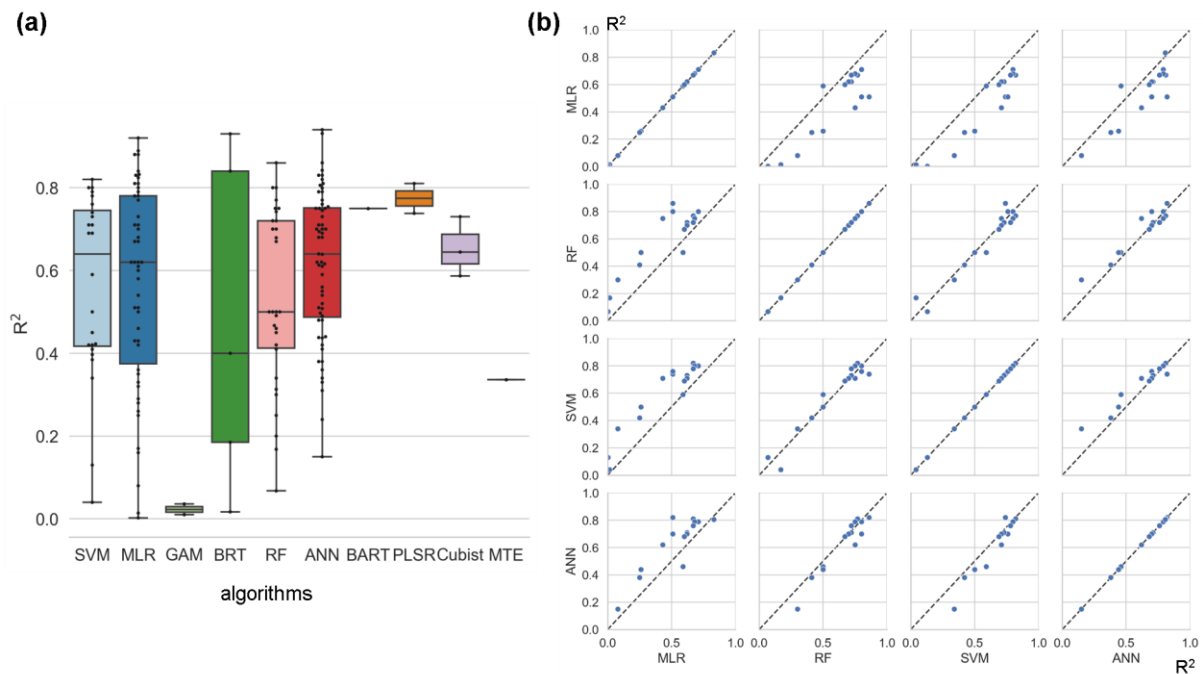
232
 233 Figure 4. The number of studies published across journals and the total number of publications per year.

234 **3.2 The formal Meta-analysis**

235 We assessed the impact of the features (e.g., algorithms, study area, PFTs, amount of data, validation methods,
 236 predictor variables, etc.) used in the different models based on differences in R-squared.

237 **3.2.1 Algorithms**

238 Among the more frequently used algorithms, ANN and SVM performed better (Fig. 5a) on average across
 239 studies (lightly better than RF). On the other hand, since cross-study comparisons of algorithm accuracy include
 240 differences in data used in model construction, we performed a pairwise comparison (Fig. 5b) of these four
 241 algorithms (i.e., ANN, SVM, RF, and MLR). In these studies, multiple models are developed for consistent
 242 training data with the interference of training data differences removed. It shows that RF and SVM perform best
 243 in the inter-study comparison (Fig. 5b). Whereas ANN performed slightly worse than RF and SVM, all three of
 244 them were stronger than MLR. Overall, the performance of RF and SVM may be good and similar in the NEE
 245 simulations.



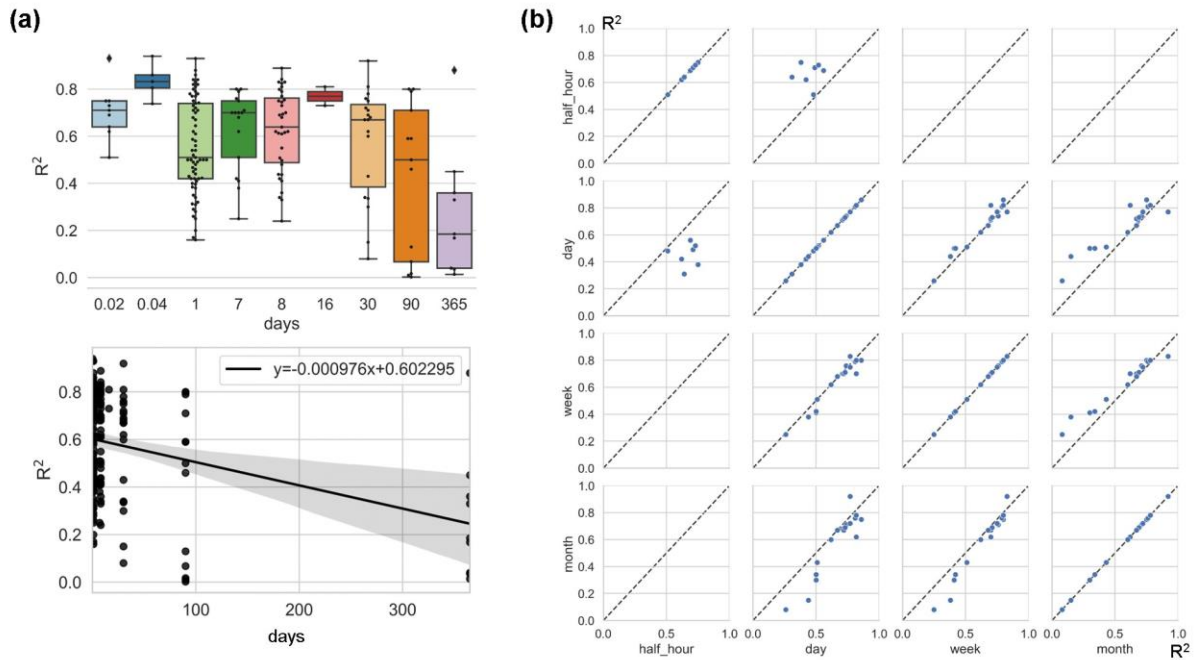
246

247 Figure 5. Differences in model accuracy (R-squared) using different algorithms across studies (a) and internal
 248 comparisons of the model accuracy (R-squared) of selected pairs of algorithms within individual studies (b).

249 Regression algorithms: Random Forests (RF), Multiple Linear Regressions (MLR), Artificial Neural Networks
 250 (ANN), Support Vector Machines (SVM), Partial Least Squares Regression (PLSR), Generalized additive
 251 model (GAM), Boosted Regression Tree (BRT), Bayesian Additive Regression Trees (BART), Cubist, model
 252 tree ensembles (MTE). In panel (a), the horizontal line in the box indicates the medians. The top and bottom
 253 border lines of the box indicate the 75% and 25% percentiles, respectively.

254 3.2.2 Time scales

255 The impact of time scale on R-squared is considerable (Fig. 6), with models with larger time scales having
 256 lower average R-squared, especially when the time scale exceeds the monthly scale. The most frequently used
 257 scales were the daily, 8-day, and monthly scales. In studies where multiple time scales were used with other
 258 characteristics being the same, we found that models with half-hourly scales were significantly more accurate
 259 than models with daily scales (Fig. 6). However, the difference in accuracy between the day-scale and week-
 260 scale models is small. The accuracy of models with a monthly scale is the lowest.



261

262

263

264

265

266

267

Figure 6. Differences in model accuracy (R-squared) at different time scales across studies with the linear regression between R-squared and time scales (a), and comparison of the model accuracy (R-squared) of selected pairs of time scales within individual studies (b). All model records were included in panel (a), while studies that used multiple time scales (with other model characteristics unchanged) were included in panel (b). Time scales: 0.02 days (half-hourly), 0.04 days (hourly), 30 days (monthly), and 90 days (quarterly).

268

3.2.3 Various predictors

269

270

271

272

273

274

275

276

277

278

Among the commonly used predictors for NEE, there are significant differences in the predictors used and their impacts on model accuracy for different PFTs (Fig. 7). Ancillary data (e.g. soil texture, soil organic content, topography) that do not have temporal variability are used less frequently because they can only explain spatial heterogeneity. In contrast, the biophysical variables LAI, FAPAR, and ET were used significantly less frequently than NDVI/EVI, especially in the cropland and wetland types. The meteorological variables T_a , R_n/R_s , and VPD were used most frequently. For forest sites, R_n/R_s and W_s appear to be the variables that improve model accuracy. For grassland sites, we found that NDVI/EVI appears to be the most effective, despite the small sample size. For sites in croplands and wetlands, we did not find predictor variables that had a significant impact on model accuracy.

279

280

281

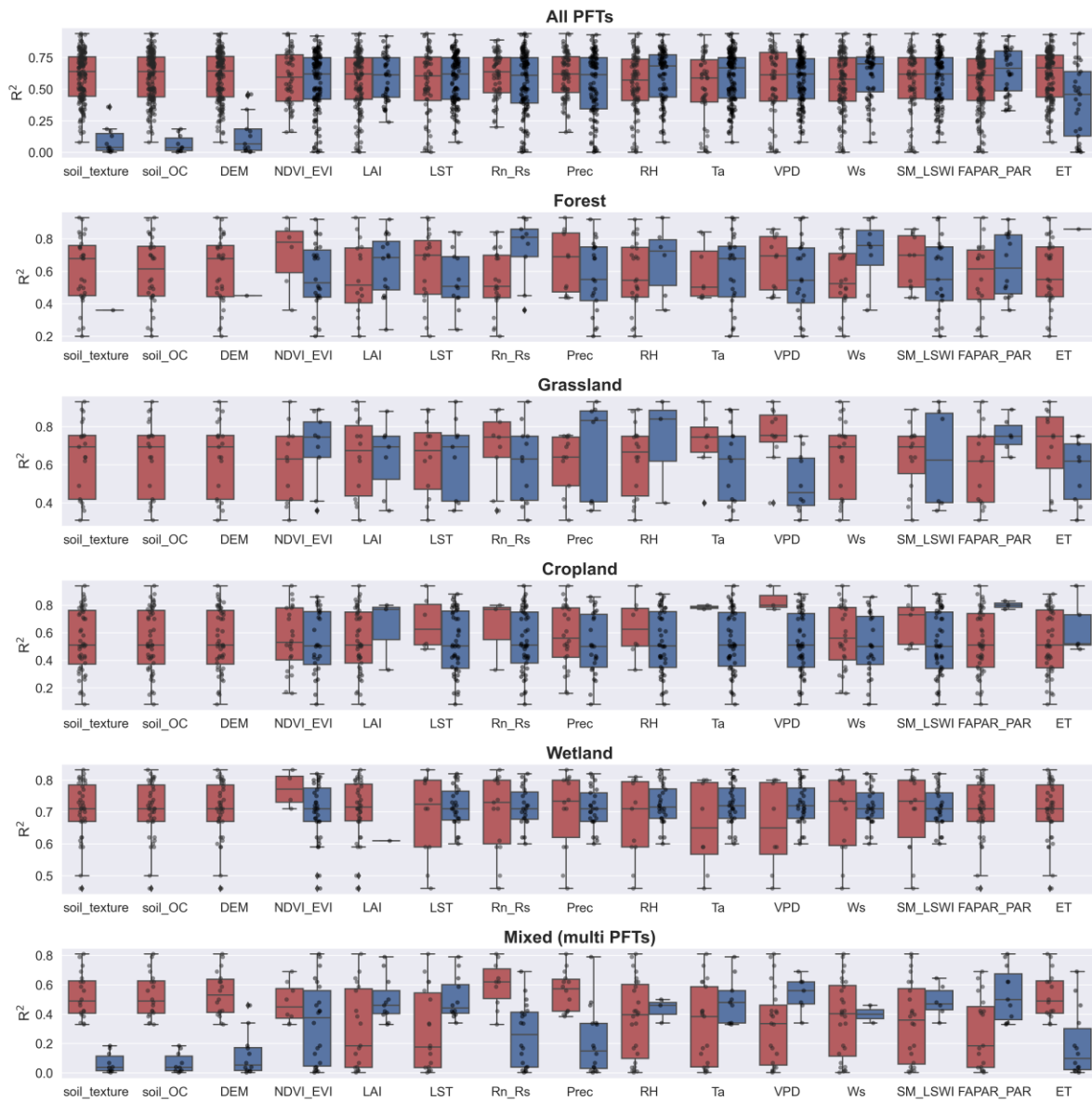
282

283

284

285

For different PFTs, the top three variables in the ranking of model importance differed (Fig. S1). SM, R_n/R_s , T_a , T_s , and VPD all showed high importance across PFTs. This suggests that the variability of measured site-scale moisture and temperature conditions is important for the simulation of NEE for all PFTs. In contrast, in the importance ranking, other variables such as precipitation and NDVI/EVI may not lead because of the lag in their effect on NEE (Hao et al., 2010; Cranko Page et al., 2022). And some other variables may improve model accuracy for specific PFTs such as groundwater table depth (GWT) for wetland sites and growing degree days (GDD) for tundra sites.



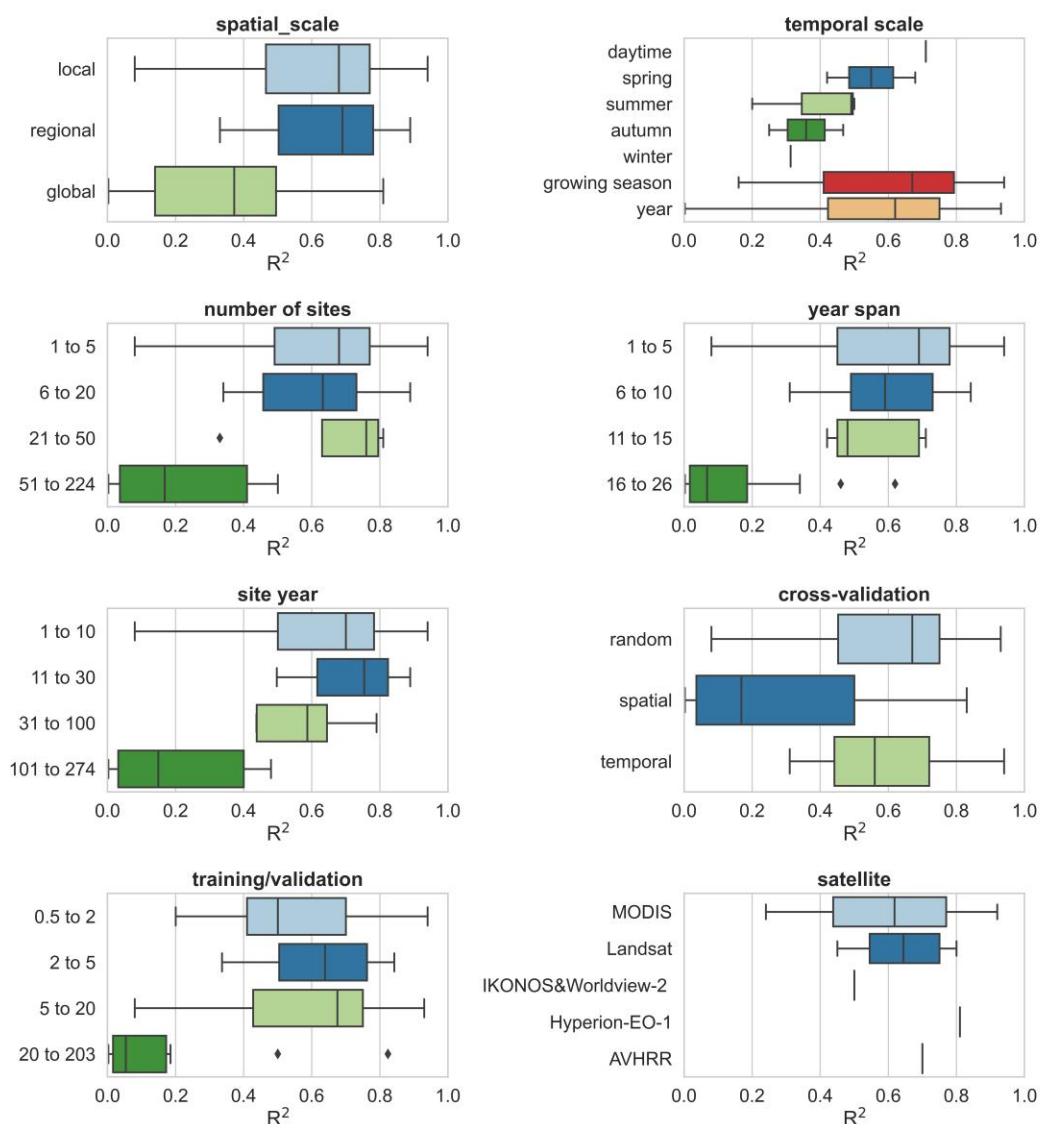
287

288 Figure 7. The impact of the various predictors incorporated in models of different PFTs (1-forest, 2-grassland, 3-
 289 cropland, 4-wetland, 6-tundra) on R-squared. Dark blue boxes indicate that the predictor was used in the model,
 290 while dark red boxes indicate that the predictor was not used. Predictors: soil organic content (Soil_OC),
 291 precipitation (Prec), soil moisture/land surface water index (SM_LSWI), net radiation/solar radiation (Rn_Rs),
 292 enhanced vegetation index (EVI), air temperature (Ta), vapor-pressure deficit (VPD), the fraction of absorbed
 293 photosynthetically active radiation/photosynthetically active radiation (FAPAR_PAR), relative humidity (RH),
 294 evapotranspiration (ET), leaf area index (LAI).

295 **3.2.4 Other features**

296 In addition, we evaluated other features of the model construction that may contribute to differences in model
 297 accuracy (Fig. 8). Studies at continental and global scales with a large number of sites and a large span of years
 298 correspond to lower R-squared than studies at local and regional scales, suggesting that studies with a large
 299 number of sites across large regions are likely to have high variability in the relationship between NEE and

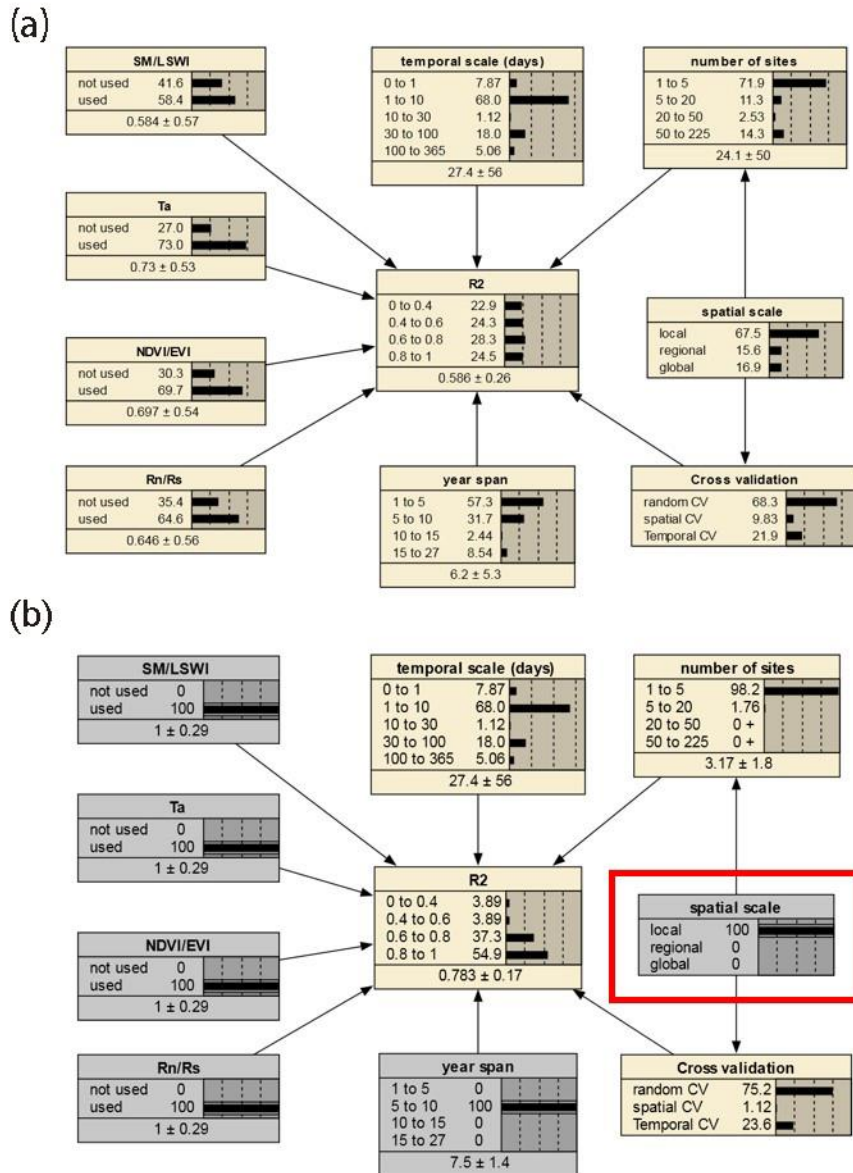
300 covariates and that studies at small scales are more likely to have higher model accuracy. Spatial validation
 301 (usually 'leave one site out') corresponds to lower model accuracy compared to random and temporal validation.
 302 This again confirms the dominant role of heterogeneity in the relationship between NEE and covariates across
 303 sites in explaining model accuracy. This seems to be indirectly supported by the fact that a high ratio of training
 304 to validation sets corresponds to a low R-squared, as this high ratio tends to be accompanied by the use of the
 305 'leave one site out' validation approach. The accuracy of the models with a growing season period was slightly
 306 higher than that of the models with an annual period. For the satellite remote sensing data used, the models
 307 based on MODIS data with biophysical variables extracted were slightly less accurate than those based on
 308 Landsat data. For the daily scale models, Landsat data performed a little better than MODIS (Fig. S2). This
 309 suggests that the higher temporal resolution of MODIS compared to Landsat may not play a dominant role in
 310 improving model accuracy. This may also be partially attributed to studies using MODIS-based explanatory data
 311 that tend to include too large surrounding areas around the site (e.g., 2x2 km), which can lead to a scale
 312 mismatch between the flux footprint and the explanatory variables.



313
 314 Figure 8. The impacts of other features (i.e. spatial scale, study period, number of sites, year span, site year,
 315 cross-validation method, training/validation, and satellite imagery) on the model performance.

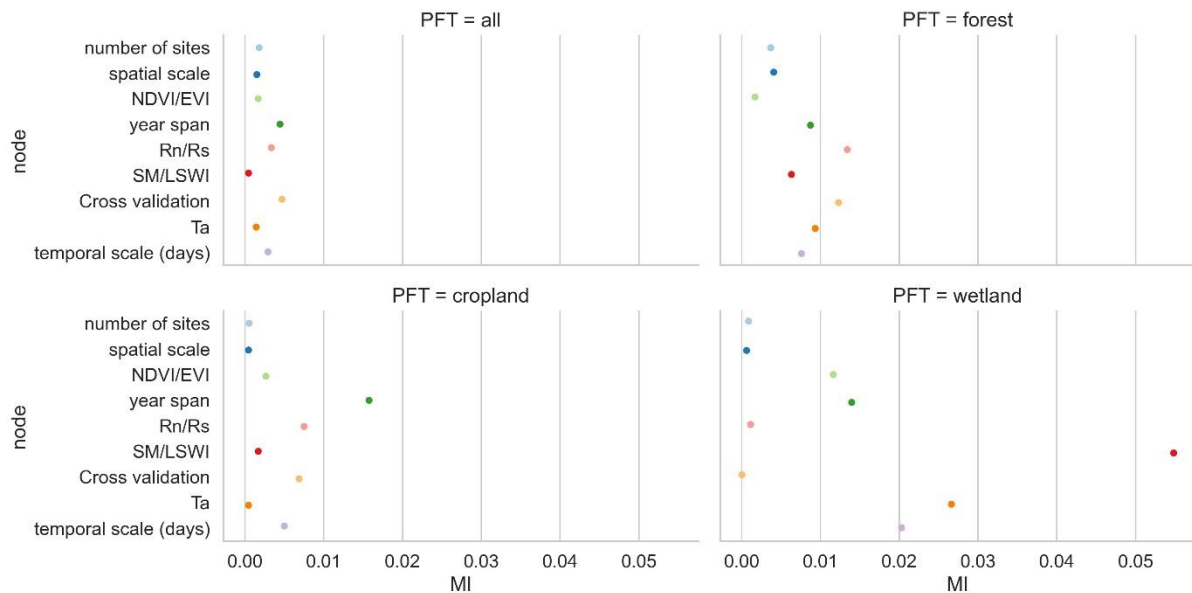
316 **3.3. The joint causal impacts of multi-features based on the BN**

317 We selected the features that had a more significant impact on model accuracy in the above assessment and
318 further incorporated them into the BN-based multivariate assessment to understand the joint impact of multiple
319 features on R-squared. The features incorporated included the spatial scale, the number of sites, the time scale,
320 the span of years, the cross-validation method, and whether some specific predictors were used. We discretized
321 the distribution of individual nodes and compiled the BN (Fig. 9.a) using records from different PFTs as input.
322 Sensitivity analysis of the R-squared node (Fig. 10) showed that R-squared was most sensitive to 'year span',
323 cross-validation method, Rn/Rs, and time scale under multi-feature control. In the forest and cropland types, R-
324 squared is more sensitive to Rn/Rs, while in the wetland type it is more sensitive to SM/LSWI and Ta. The
325 sensitivity of R-squared to 'year span' was much higher in the cropland type compared to the other PFTs, which
326 may suggest that the interannual variability in the NEE simulations of the cropland type is higher due to
327 potential interannual variability of the planting structure and irrigation practices. For the cropland type,
328 differences in the phenology, harvesting, and irrigation (water volume and frequency) in different years can lead
329 to significant inter-annual differences in NEE simulations. Subsequently, using the constructed BN (with the
330 empirical information in previous studies incorporated), for new studies we can instructively infer the
331 probability distribution of the possible R-squared (Fig. 9.b) with some model features predetermined. In
332 previous studies, spatio-temporal mapping of NEE based on statistical models has often lacked accuracy
333 assessment since there are no grid-scale NEE observations, and this BN may have the potential to be used to
334 validate the accuracy (R-squared) of the NEE time series output of the grid-scale (i.e. inferring possible R-
335 squared from model features, where the output of the grid-scale is considered to be of the form 'leave one site
336 out').



337
 338
 339
 340
 341
 342
 343
 344
 345

Figure 9. The joint effects of multiple features on the R-squared based on the BN with all records input (a) and the inference on the probability distribution of R-squared based on the BN with the status of some nodes determined (b). The values before and after the “±” indicate the mean and standard deviation of the distribution, respectively. The gray boxes indicate that the status of the nodes has been determined. In panel (b), specific values of parent nodes such as ‘spatial scale’ are determined (shown in the red box), leading to an increase in the expected R-squared compared to the average scenario of the panel (a) (as inferred from the posterior conditional probabilities with the status of the node ‘spatial scale’ are determined as ‘local’).



346

347 Figure 10. The sensitivity analysis of the R-squared node to other nodes based on the mutual information (MI)
 348 across PFTs. ‘Cross-validation’ is the cross-validation method including spatial, temporal, and random cross-
 349 validation.

350 4 Discussions

351 Many studies have evaluated the incorporation of various predictors and model features using machine learning
 352 for improving the site-scale NEE predictions (Tramontana et al., 2016; Zeng et al., 2020; Jung et al., 2011). A
 353 comprehensive evaluation of these studies to provide definitive guidance on the selection of features in NEE
 354 prediction modeling is limited. This study fills the research gap with a meta-analysis of the literature through
 355 statistics on the accuracy and performance of models. Machine learning-based NEE simulations and predictions
 356 still suffer from high uncertainty. By better understanding the expected improvements that can be achieved
 357 through the inclusion of different features, we can identify priorities for the consideration of different features in
 358 modeling efforts and avoid operations decreasing model accuracy.

359

360 Compared to previous comparisons of machine learning-based NEE prediction models, this study is more
 361 comprehensive. Previous studies (Abbasian et al., 2022) have also found advantages of RF over other
 362 algorithms in NEE prediction. This study consolidated this finding using a larger amount of evidence. Previous
 363 studies (Tramontana et al., 2016) have also compared the impact of different practices in NEE prediction models
 364 based on the R-squared, such as comparing the difference in accuracy between the two predictor combinations
 365 (i.e., using only remotely sensed data and using remotely sensed data and meteorological data together). In
 366 contrast, since this study incorporated more detailed factors influencing model accuracy, the understanding of
 367 such issues was deepened. However, there are still many uncertainties and challenges in NEE prediction not
 368 clarified in this study.

369 **4.1 Challenges in the site-scale NEE simulation and implications for other carbon flux simulations**

370 **4.1.1 Variations in time scales**

371 In the above analysis, we found that the effect of the time scale of the model is considerable. This suggests that
372 we should be careful in determining the time scale of the model to consider whether the predictor variables used
373 will work at this time scale. Previous studies have reported the dependence of the NEE variability and
374 mechanism on the time scales. On the one hand, the importance of variables affecting NEE varies at different
375 time scales. For example, in tropical and subtropical forests in southern China (Yan et al., 2013), seasonal NEE
376 variability is predominantly controlled by soil temperature and moisture, while interannual NEE variability is
377 controlled by the annual precipitation variation. A study (Jung et al., 2017) showed that for annual-scale NEE
378 variability, water availability and temperature were the dominant drivers at the local and global scales,
379 respectively. This indicates the need to recognize the temporal and spatial driving mechanisms of NEE in
380 advance in the development of NEE prediction models. On the other hand, dependence may exist between NEE
381 anomalies at various time scales. For example, previous studies (Luyssaert et al., 2007) showed that short-term
382 temperature anomalies may interpret both the daily and seasonal NEE anomalies. This implies that the models at
383 different time scales may not be independent. In the previous studies, the relationship between prediction
384 models at different scales has not been well investigated, and it may be valuable to compare the relations
385 between data and models at different scales in depth. Larger time scales correspond to lower model accuracy,
386 possibly related to the fact that some small-time-scale relations between NEE and covariates (especially
387 meteorological variables) are smoothed. In particular, for models with time scales smaller than one day (e.g.
388 half-hourly models), the 8-daily and 16-daily biophysical variable data obtained from satellite remote sensing
389 are difficult to explain the temporal variation in the sub-daily NEE. Therefore, for models at small time scales
390 (i.e. half-hourly, hourly, daily scale models), in situ meteorological variables may be more important. The
391 inclusion of some ancillary variables (e.g. soil texture, topographic variables) with no temporal dynamic
392 information may be ineffective unless many sites are included in the model and the spatial variability of the
393 ancillary variables for these sites is sufficiently large (Virkkala et al., 2021).

394

395 In terms of completeness and purity of training data, hourly and daily models can be better compared to monthly
396 and yearly models. Hourly and daily models can usually preclude those low-quality data and gaps in the flux
397 observations. However, for monthly and yearly scale models, gap-filling (Ruppert et al., 2006; Moffat et al.,
398 2007; Zhu et al., 2022) is necessary because there are few complete and continuous fluxes observations without
399 data gaps on the monthly to yearly scales. Since various gap-filling techniques rely on environmental factors
400 (Moffat et al., 2007) such as meteorological observations, this may introduce uncertainty in the predictive
401 models (i.e., a small fraction of the observed information of NEE is estimated from a combination of
402 independent variables). How it would affect the accuracy of prediction models at various time scales remains
403 uncertain, although various gap-filling techniques have been widely used in the pre-processing of training data.

404

405 In addition, the impacts of lagged effects (Hao et al., 2010; Cranko Page et al., 2022) of covariates are not
406 considered in most models, which may underestimate the degree of explanation of NEE for some predictor
407 variables (e.g. precipitation). Most of the machine learning-based models use only the average Ta and do not
408 take into account the maximum temperature, minimum temperature, daily difference in temperature, etc., as in

409 the process-based ecological models (Mitchell et al., 2009). This suggests that the inclusion of different
410 temporal characteristics of individual variables in machine learning-based NEE prediction models may be
411 insufficient.

412 **4.1.2 Scale mismatch of explanatory predictors and flux footprints**

413 An excessively large extraction area of remote sensing data (e.g., 2x2 km) may be inappropriate. In the non-
414 homogeneous underlying conditions, the agreement of the area of flux footprints with the scale of the predictors
415 should be considered in the extraction of the predictor variables in various PFTs (Chu et al., 2021).

416

417 The effects of this mismatch between explanatory variables and flux footprints may be diverse for different
418 PFTs. For example, for cropland types, the NEE is monitored at a range of several hundred meters around the
419 flux towers, but remote sensing variables such as FAPAR, NDVI, LAI, etc. can be extracted at coarse scales
420 (e.g., 2x2 km), some effects outside the extent of the flux footprint (Chu et al., 2021; Walther et al., 2021) are
421 incorporated (e.g., planting structures with high spatial heterogeneity, agricultural practices such as irrigation).
422 And for more homogeneous types such as grasslands, coarse-scale meteorological data may still cause spatial
423 mismatches, even though the differences in land cover types within the 2x2 km and 200x200 m extent around
424 the flux stations in grasslands may not be considerable. For example, precipitation with high spatial
425 heterogeneity can dominate the spatial variability of soil moisture and thus affect the spatial variability of
426 grassland NEE (Wu et al., 2011; Jongen et al., 2011). However, using 0.25°x0.25° reanalysis precipitation data
427 (Zeng et al., 2020) may make it difficult for predictive models to capture this spatial heterogeneity around the
428 flux station.

429

430 Since few of the studies included in this meta-analysis considered the effect of variation in flux footprint, this
431 feature was difficult to consider in this study. However, its influence should still be further investigated in future
432 studies. With flux footprints calculated (Kljun et al., 2015) and the factors around the flux site (Walther et al.,
433 2021) that affect the flux footprint incorporated, it is promising to clarify this issue.

434 **4.1.3 Possible unbalance of training and validation sets**

435 In addition to the time scale of the models, the most significant differences in model accuracy and performance
436 were found in the heterogeneity within the NEE dataset and the match of the training set and validation set.

437 Often NEE simulations can achieve high accuracy in local studies, where the main factor negatively affecting
438 model accuracy may be the interannual variability in the relationship between NEE and covariates. However,
439 the complexity may increase when the dataset contains a large study area, many sites, PFTs, and year spans.

440 Under this condition, the accuracy of the model in the 'leave one site out' validation may be more dependent on
441 the correlation and match between the training and validation sets (Jung et al., 2020). When the model is applied
442 to an outlier site (of which the NEE, covariates, and their relationship are very different compared with the
443 remaining sites), it appears to be difficult to achieve a high prediction accuracy (Jung et al., 2020). If we further
444 upscale the prediction model to large spatial and time scales, the uncertainties involved may be difficult to
445 assess (Zeng et al., 2020). We can only infer the possible model accuracy based on the similarity of the
446 distribution of predictors in the predicted grid to that of the existing sites in the model. In the upscaling process,

447 reanalysis data with the coarse spatial resolution are often used as an alternative for site-scale meteorological
448 predictors. However, most studies did not assess in detail the possible errors associated with spatial mismatches
449 in this operation.

450

451 In summary, the site-scale NEE predictions may require more focus on the internal heterogeneity of the NEE
452 dataset and the matching of the training set and validation set, and also require a better understanding of the
453 influence of different scales of the same variable (e.g. site-scale precipitation and grid-scale precipitation in the
454 reanalysis meteorological data) across modeling and upscaling steps. For the prediction of other carbon fluxes
455 such as methane fluxes (in the same framework as the NEE predictions), the results of this study may also be
456 partially applicable, although there may be significant differences in the use of specific predictors (Peltola et al.,
457 2019).

458 **4.2 Uncertainties**

459 The uncertainties in this analysis may include:

- 460 a) **Publication bias and weighting:** Publication bias is not refined due to the limitations of the number of
461 articles that can be included. Meta-analyses often measure the quality of journals and the data availability
462 (Borenstein et al., 2011; Field and Gillett, 2010) to determine the weighting of the literature in a
463 comprehensive assessment. However, a high proportion of the articles in this study did not make flux
464 observations publicly available or share the NEE prediction models developed. Furthermore, meta-analysis
465 studies in other fields typically measure the impact of papers by evidence/data volume, and the variance of
466 the evaluated effects (Adams et al., 1997; Don et al., 2011; Liu et al., 2018). However, in this study,
467 because no convincing method is found to quantify the weights of results from included articles, some
468 features (e.g. the number of flux sites, the span of years) were directly assessed rather than used to
469 determine the weights of the articles.
- 470 b) **Limitations of the criteria for inclusion in the literature:** in the model accuracy-based evaluation, we
471 selected only literature that developed multiple regression models. Potentially valuable information from
472 univariate regression models was not included. In addition, only papers in high-quality English journals
473 were included in this study to control for possible errors due to publication bias. However, many studies
474 that fit this theme may have been published in other languages or other journals.
- 475 c) **Independence between features:** There is dependence between the evaluated features (e.g. the dependency
476 between the spatial extent and the number of sites). It may negatively affect the assessment of the impact
477 of individual features on the accuracy of the model, although the BN-based analysis of joint effects can
478 reduce the impact of this dependence between variables by specifying causal relationships between
479 features. The interference of unknown dependencies between features may still not be eliminated when we
480 focus on the effects of an individual feature on the model performance. We should pay more attention to
481 the effect of features on model accuracy individually in future studies, and it may be valuable to keep other
482 features as constants while changing the level of only one feature and assessing the difference. It may help
483 us to understand the real sensitivity of model accuracy to different features in specific conditions. The
484 sample size collected in this study (178 records in total) is not very large. This also suggests that more
485 future efforts should be devoted to the comprehensive evaluation and summarization of NEE simulations.

486
487
488
489
490

491

492
493
494
495
496
497
498
499
500
501
502
503
504
505
506
507

Additionally, there are still other potential factors not considered by this study such as the uncertainty of climate data (site vs reanalysis), footprint matching between site and satellite images, etc. Overall, although the quantitative results of this study should be used with caution, they still have positive implications for guiding future such studies.

5 Conclusion

We performed a meta-analysis of the site-scale NEE simulations combining in situ flux observations, meteorological, biophysical, and ancillary predictors, and machine learning. The impacts of various features throughout the modeling process on the accuracy of the model were evaluated. The main findings of this study include:

1. RF and SVM performed better than other evaluated algorithms.
2. The impact of time scale on model performance is significant. Models with larger time scales have lower average R-squared, especially when the time scale exceeds the monthly scale. Models with half-hourly scales (average R-squared = 0.73) were significantly more accurate than models with daily scales (average R-squared = 0.5).
3. Among the commonly used predictors for NEE, there are significant differences in the predictors used and their impacts on model accuracy for different PFTs.
4. It is necessary to focus on the potential imbalance between the training and validation sets in NEE simulations. Studies at continental and global scales (average R-squared = 0.37) with multiple PFTs, more sites, and a large span of years correspond to lower R-squared than studies at local (average R-squared = 0.69) and regional scales (average R-squared = 0.7).

508 **Acknowledgments**

509 We thank the editors and three anonymous referees for their insightful comments on this paper which
510 substantially improved.

511 **Financial support**

512 This research was supported by the National Natural Science Foundation of China (Grant No. U1803243), the
513 Key projects of the Natural Science Foundation of Xinjiang Autonomous Region (Grant No. 2022D01D01), the
514 Strategic Priority Research Program of the Chinese Academy of Sciences (Grant No. XDA20060302), and
515 High-End Foreign Experts Project.

516 **Author contributions**

517 H.S and G.L initiated this research and were responsible for the integrity of the work as a whole. H.S performed
518 formal analysis, and calculations and drafted the manuscript. H.S, G.L, X.M, X.Y, Y.W, W.Z, M.X, C.Z, and
519 Y.Z were responsible for the data collection and analysis. G.L, P.D.M, T.V.D.V, O.H, and A.K contributed
520 resources and financial support.

521 **Competing interests**

522 The authors declare that they have no conflict of interest.

523 **Data availability**

524 The data used in this study can be accessed by contacting the first author (shihaiyang16@mails.ucas.ac.cn)
525 based on a reasonable request.

526 **Code availability**

527 The code used in this study can be accessed by contacting the first author (shihaiyang16@mails.ucas.ac.cn)
528 based on a reasonable request.

529

530

531 **References**

- 532 Abbasian, H., Solgi, E., Mohsen Hosseini, S., and Hossein Kia, S.: Modeling terrestrial net ecosystem
533 exchange using machine learning techniques based on flux tower measurements, *Ecological*
534 *Modelling*, 466, 109901, <https://doi.org/10.1016/j.ecolmodel.2022.109901>, 2022.
- 535 Adams, D. C., Gurevitch, J., and Rosenberg, M. S.: Resampling tests for meta - analysis of ecological
536 data, *Ecology*, 78, 1277–1283, 1997.
- 537 Baldocchi, D. D.: Assessing the eddy covariance technique for evaluating carbon dioxide exchange
538 rates of ecosystems: past, present and future, 9, 479–492, [https://doi.org/10.1046/j.1365-](https://doi.org/10.1046/j.1365-2486.2003.00629.x)
539 [2486.2003.00629.x](https://doi.org/10.1046/j.1365-2486.2003.00629.x), 2003.
- 540 Berryman, E. M., Vanderhoof, M. K., Bradford, J. B., Hawbaker, T. J., Henne, P. D., Burns, S. P.,
541 Frank, J. M., Birdsey, R. A., and Ryan, M. G.: Estimating soil respiration in a subalpine landscape
542 using point, terrain, climate, and greenness data, *Journal of Geophysical Research: Biogeosciences*,
543 123, 3231–3249, 2018.
- 544 Borenstein, M., Hedges, L. V., Higgins, J. P., and Rothstein, H. R.: *Introduction to meta-analysis*,
545 John Wiley & Sons, 2011.
- 546 Cho, S., Kang, M., Ichii, K., Kim, J., Lim, J.-H., Chun, J.-H., Park, C.-W., Kim, H. S., Choi, S.-W.,
547 and Lee, S.-H.: Evaluation of forest carbon uptake in South Korea using the national flux tower
548 network, remote sensing, and data-driven technology, *Agricultural and Forest Meteorology*, 311,
549 108653, 2021.
- 550 Chu, H., Luo, X., Ouyang, Z., Chan, W. S., Dengel, S., Biraud, S. C., Torn, M. S., Metzger, S.,
551 Kumar, J., Arain, M. A., Arkebauer, T. J., Baldocchi, D., Bernacchi, C., Billesbach, D., Black, T. A.,
552 Blanken, P. D., Bohrer, G., Bracho, R., Brown, S., Brunzell, N. A., Chen, J., Chen, X., Clark, K.,
553 Desai, A. R., Duman, T., Durden, D., Fares, S., Forbrich, I., Gamon, J. A., Gough, C. M., Griffis, T.,
554 Helbig, M., Hollinger, D., Humphreys, E., Ikawa, H., Iwata, H., Ju, Y., Knowles, J. F., Knox, S. H.,
555 Kobayashi, H., Kolb, T., Law, B., Lee, X., Litvak, M., Liu, H., Munger, J. W., Noormets, A., Novick,
556 K., Oberbauer, S. F., Oechel, W., Oikawa, P., Papuga, S. A., Pendall, E., Prajapati, P., Prueger, J.,
557 Quinton, W. L., Richardson, A. D., Russell, E. S., Scott, R. L., Starr, G., Staebler, R., Stoy, P. C.,
558 Stuart-Haëntjens, E., Sonntag, O., Sullivan, R. C., Suyker, A., Ueyama, M., Vargas, R., Wood, J.
559 D., and Zona, D.: Representativeness of Eddy-Covariance flux footprints for areas surrounding
560 AmeriFlux sites, *Agricultural and Forest Meteorology*, 301–302, 108350,
561 <https://doi.org/10.1016/j.agrformet.2021.108350>, 2021.
- 562 Cleverly, J., Vote, C., Isaac, P., Ewenz, C., Harahap, M., Beringer, J., Campbell, D. I., Daly, E.,
563 Eamus, D., He, L., Hunt, J., Grace, P., Hutley, L. B., Laubach, J., McCaskill, M., Rowlings, D.,
564 Rutledge Jonker, S., Schipper, L. A., Schroder, I., Teodosio, B., Yu, Q., Ward, P. R., Walker, J. P.,
565 Webb, J. A., and Grover, S. P. P.: Carbon, water and energy fluxes in agricultural systems of
566 Australia and New Zealand, 287, <https://doi.org/10.1016/j.agrformet.2020.107934>, 2020.
- 567 Cranko Page, J., De Kauwe, M. G., Abramowitz, G., Cleverly, J., Hinko-Najera, N., Hovenden, M. J.,
568 Liu, Y., Pitman, A. J., and Ogle, K.: Examining the role of environmental memory in the
569 predictability of carbon and water fluxes across Australian ecosystems, *Biogeosciences*, 19, 1913–
570 1932, 2022.
- 571 Cui, X., Goff, T., Cui, S., Menefee, D., Wu, Q., Rajan, N., Nair, S., Phillips, N., and Walker, F.:
572 Predicting carbon and water vapor fluxes using machine learning and novel feature ranking
573 algorithms, *Science of The Total Environment*, 775, 145130, 2021.

574 Don, A., Schumacher, J., and Freibauer, A.: Impact of tropical land-use change on soil organic carbon
575 stocks – a meta-analysis, 17, 1658–1670, <https://doi.org/10.1111/j.1365-2486.2010.02336.x>, 2011.

576 Field, A. P. and Gillett, R.: How to do a meta - analysis, *British Journal of Mathematical and*
577 *Statistical Psychology*, 63, 665–694, 2010.

578 Fu, D., Chen, B., Zhang, H., Wang, J., Black, T. A., Amiro, B. D., Bohrer, G., Bolstad, P., Coulter,
579 R., and Rahman, A. F.: Estimating landscape net ecosystem exchange at high spatial–temporal
580 resolution based on Landsat data, an improved upscaling model framework, and eddy covariance flux
581 measurements, *Remote Sensing of Environment*, 141, 90–104, 2014.

582 Fu, Z., Stoy, P. C., Poulter, B., Gerken, T., Zhang, Z., Wakkulcho, G., and Niu, S.: Maximum carbon
583 uptake rate dominates the interannual variability of global net ecosystem exchange, *Global Change*
584 *Biology*, 25, 3381–3394, 2019.

585 Hao, Y., Wang, Y., Mei, X., and Cui, X.: The response of ecosystem CO₂ exchange to small
586 precipitation pulses over a temperate steppe, *Plant Ecol*, 209, 335–347,
587 <https://doi.org/10.1007/s11258-010-9766-1>, 2010.

588 Harris, N. L., Gibbs, D. A., Baccini, A., Birdsey, R. A., de Bruin, S., Farina, M., Fatoyinbo, L.,
589 Hansen, M. C., Herold, M., Houghton, R. A., Potapov, P. V., Suarez, D. R., Roman-Cuesta, R. M.,
590 Saatchi, S. S., Slay, C. M., Turubanova, S. A., and Tyukavina, A.: Global maps of twenty-first
591 century forest carbon fluxes, *Nat. Clim. Chang.*, 11, 234–240, [https://doi.org/10.1038/s41558-020-](https://doi.org/10.1038/s41558-020-00976-6)
592 [00976-6](https://doi.org/10.1038/s41558-020-00976-6), 2021.

593 Huemmrich, K. F., Campbell, P., Landis, D., and Middleton, E.: Developing a common globally
594 applicable method for optical remote sensing of ecosystem light use efficiency, *Remote Sensing of*
595 *Environment*, 230, 111190, 2019.

596 Jongen, M., Pereira, J. S., Aires, L. M. I., and Pio, C. A.: The effects of drought and timing of
597 precipitation on the inter-annual variation in ecosystem-atmosphere exchange in a Mediterranean
598 grassland, *Agricultural and Forest Meteorology*, 151, 595–606,
599 <https://doi.org/10.1016/j.agrformet.2011.01.008>, 2011.

600 Jung, M., Reichstein, M., Margolis, H. A., Cescatti, A., Richardson, A. D., Arain, M. A., Arneth, A.,
601 Bernhofer, C., Bonal, D., and Chen, J.: Global patterns of land - atmosphere fluxes of carbon dioxide,
602 latent heat, and sensible heat derived from eddy covariance, satellite, and meteorological observations,
603 *Journal of Geophysical Research: Biogeosciences*, 116, 2011.

604 Jung, M., Reichstein, M., Schwalm, C. R., Huntingford, C., Sitch, S., Ahlström, A., Arneth, A.,
605 Camps-Valls, G., Ciais, P., Friedlingstein, P., Gans, F., Ichii, K., Jain, A. K., Kato, E., Papale, D.,
606 Poulter, B., Raduly, B., Rödenbeck, C., Tramontana, G., Viovy, N., Wang, Y.-P., Weber, U., Zaehle,
607 S., and Zeng, N.: Compensatory water effects link yearly global land CO₂ sink changes to
608 temperature, 541, 516–520, <https://doi.org/10.1038/nature20780>, 2017.

609 Jung, M., Schwalm, C., Migliavacca, M., Walther, S., Camps-Valls, G., Koirala, S., Anthoni, P.,
610 Besnard, S., Bodesheim, P., Carvalhais, N., Chevallier, F., Gans, F., S Goll, D., Haverd, V., Köhler,
611 P., Ichii, K., K Jain, A., Liu, J., Lombardozzi, D., E M S Nabel, J., A Nelson, J., O’Sullivan, M.,
612 Pallandt, M., Papale, D., Peters, W., Pongratz, J., Rödenbeck, C., Sitch, S., Tramontana, G., Walker,
613 A., Weber, U., and Reichstein, M.: Scaling carbon fluxes from eddy covariance sites to globe:
614 Synthesis and evaluation of the FLUXCOM approach, 17, 1343–1365, [https://doi.org/10.5194/bg-17-](https://doi.org/10.5194/bg-17-1343-2020)
615 [1343-2020](https://doi.org/10.5194/bg-17-1343-2020), 2020.

- 616 Kaur, H., Pannu, H. S., and Malhi, A. K.: A Systematic Review on Imbalanced Data Challenges in
617 Machine Learning: Applications and Solutions, *ACM Comput. Surv.*, 52, 79:1-79:36,
618 <https://doi.org/10.1145/3343440>, 2019.
- 619 Kljun, N., Calanca, P., Rotach, M., and Schmid, H. P.: A simple two-dimensional parameterisation for
620 Flux Footprint Prediction (FFP), *Geoscientific Model Development*, 8, 3695–3713, 2015.
- 621 Liu, Q., Zhang, Y., Liu, B., Amonette, J. E., Lin, Z., Liu, G., Ambus, P., and Xie, Z.: How does
622 biochar influence soil N cycle? A meta-analysis, *Plant and soil*, 426, 211–225, 2018.
- 623 Luysaert, S., Janssens, I. A., Sulkava, M., Papale, D., Dolman, A. J., Reichstein, M., Hollmén, J.,
624 Martin, J. G., Suni, T., Vesala, T., Loustau, D., Law, B. E., and Moors, E. J.: Photosynthesis drives
625 anomalies in net carbon-exchange of pine forests at different latitudes, 13, 2110–2127,
626 <https://doi.org/10.1111/j.1365-2486.2007.01432.x>, 2007.
- 627 Marcot, B. G. and Hanea, A. M.: What is an optimal value of k in k-fold cross-validation in discrete
628 Bayesian network analysis?, *Comput Stat*, 36, 2009–2031, [https://doi.org/10.1007/s00180-020-00999-](https://doi.org/10.1007/s00180-020-00999-9)
629 9, 2021.
- 630 Mitchell, S., Beven, K., and Freer, J.: Multiple sources of predictive uncertainty in modeled estimates
631 of net ecosystem CO₂ exchange, *Ecological Modelling*, 220, 3259–3270,
632 <https://doi.org/10.1016/j.ecolmodel.2009.08.021>, 2009.
- 633 Moffat, A. M., Papale, D., Reichstein, M., Hollinger, D. Y., Richardson, A. D., Barr, A. G.,
634 Beckstein, C., Braswell, B. H., Churkina, G., Desai, A. R., Falge, E., Gove, J. H., Heimann, M., Hui,
635 D., Jarvis, A. J., Kattge, J., Noormets, A., and Stauch, V. J.: Comprehensive comparison of gap-filling
636 techniques for eddy covariance net carbon fluxes, 147, 209–232,
637 <https://doi.org/10.1016/j.agrformet.2007.08.011>, 2007.
- 638 Moffat, A. M., Beckstein, C., Churkina, G., Mund, M., and Heimann, M.: Characterization of
639 ecosystem responses to climatic controls using artificial neural networks, 16, 2737–2749,
640 <https://doi.org/10.1111/j.1365-2486.2010.02171.x>, 2010.
- 641 Moher, D., Liberati, A., Tetzlaff, J., Altman, D. G., and Prisma Group: Preferred reporting items for
642 systematic reviews and meta-analyses: the PRISMA statement, *PLoS medicine*, 6, e1000097, 2009.
- 643 Moon, T. K.: The expectation-maximization algorithm, 13, 47–60, 1996.
- 644 Papale, D. and Valentini, R.: A new assessment of European forests carbon exchanges by eddy fluxes
645 and artificial neural network spatialization, 9, 525–535, [https://doi.org/10.1046/j.1365-](https://doi.org/10.1046/j.1365-2486.2003.00609.x)
646 2486.2003.00609.x, 2003.
- 647 Park, S.-B., Knohl, A., Lucas-Moffat, A. M., Migliavacca, M., Gerbig, C., Vesala, T., Peltola, O.,
648 Mammarella, I., Kolle, O., Lavrič, J. V., Prokushkin, A., and Heimann, M.: Strong radiative effect
649 induced by clouds and smoke on forest net ecosystem productivity in central Siberia, *Agricultural and*
650 *Forest Meteorology*, 250–251, 376–387, <https://doi.org/10.1016/j.agrformet.2017.09.009>, 2018.
- 651 Pearl, J.: Bayesian networks: A model of self-activated memory for evidential reasoning, in:
652 *Proceedings of the 7th Conference of the Cognitive Science Society*, University of California, Irvine,
653 CA, USA, 15–17, 1985.
- 654 Peltola, O., Vesala, T., Gao, Y., Rätty, O., Alekseychik, P., Aurela, M., Chojnicki, B., Desai, A. R.,
655 Dolman, A. J., Euskirchen, E. S., Friborg, T., Göckede, M., Helbig, M., Humphreys, E., Jackson, R.
656 B., Jocher, G., Joos, F., Klatt, J., Knox, S. H., Kowalska, N., Kutzbach, L., Lienert, S., Lohila, A.,
657 Mammarella, I., Nadeau, D. F., Nilsson, M. B., Oechel, W. C., Peichl, M., Pypker, T., Quinton, W.,

658 Rinne, J., Sachs, T., Samson, M., Schmid, H. P., Sonnentag, O., Wille, C., Zona, D., and Aalto, T.:
659 Monthly gridded data product of northern wetland methane emissions based on upscaling eddy
660 covariance observations, *Earth System Science Data*, 11, 1263–1289, [https://doi.org/10.5194/essd-11-](https://doi.org/10.5194/essd-11-1263-2019)
661 1263-2019, 2019.

662 Reed, D. E., Poe, J., Abraha, M., Dahlin, K. M., and Chen, J.: Modeled Surface-Atmosphere Fluxes
663 From Paired Sites in the Upper Great Lakes Region Using Neural Networks, *Journal of Geophysical*
664 *Research: Biogeosciences*, 126, <https://doi.org/10.1029/2021JG006363>, 2021.

665 Reichstein, M., Camps-Valls, G., Stevens, B., Jung, M., Denzler, J., Carvalhais, N., and Prabhat:
666 Deep learning and process understanding for data-driven Earth system science, 566, 195–204,
667 <https://doi.org/10.1038/s41586-019-0912-1>, 2019.

668 Reitz, O., Graf, A., Schmidt, M., Ketzler, G., and Leuchner, M.: Upscaling Net Ecosystem Exchange
669 Over Heterogeneous Landscapes With Machine Learning, 126, e2020JG005814,
670 <https://doi.org/10.1029/2020JG005814>, 2021.

671 Ruppert, J., Mauder, M., Thomas, C., and Lüers, J.: Innovative gap-filling strategy for annual sums of
672 CO₂ net ecosystem exchange, 138, 5–18, <https://doi.org/10.1016/j.agrformet.2006.03.003>, 2006.

673 Shi, H., Luo, G., Zheng, H., Chen, C., Bai, J., Liu, T., Ochege, F. U., and De Maeyer, P.: Coupling the
674 water-energy-food-ecology nexus into a Bayesian network for water resources analysis and
675 management in the Syr Darya River basin, *Journal of Hydrology*, 581, 124387,
676 <https://doi.org/10.1016/j.jhydrol.2019.124387>, 2020.

677 Shi, H., Hellwich, O., Luo, G., Chen, C., He, H., Ochege, F. U., Van de Voorde, T., Kurban, A., and
678 de Maeyer, P.: A global meta-analysis of soil salinity prediction integrating satellite remote sensing,
679 soil sampling, and machine learning, 1–15, <https://doi.org/10.1109/TGRS.2021.3109819>, 2021.

680 Tian, X., Yan, M., van der Tol, C., Li, Z., Su, Z., Chen, E., Li, X., Li, L., Wang, X., Pan, X., Gao, L.,
681 and Han, Z.: Modeling forest above-ground biomass dynamics using multi-source data and
682 incorporated models: A case study over the qilian mountains, *Agricultural and Forest Meteorology*,
683 246, 1–14, <https://doi.org/10.1016/j.agrformet.2017.05.026>, 2017.

684 Tramontana, G., Jung, M., Schwalm, C. R., Ichii, K., Camps-Valls, G., Ráduly, B., Reichstein, M.,
685 Arain, M. A., Cescatti, A., Kiely, G., Merbold, L., Serrano-Ortiz, P., Sickert, S., Wolf, S., and Papale,
686 D.: Predicting carbon dioxide and energy fluxes across global FLUXNET sites with regression
687 algorithms, *Biogeosciences*, 13, 4291–4313, <https://doi.org/10.5194/bg-13-4291-2016>, 2016.

688 Van Hulse, J., Khoshgoftaar, T. M., and Napolitano, A.: Experimental perspectives on learning from
689 imbalanced data, in: *Proceedings of the 24th international conference on Machine learning*, New
690 York, NY, USA, 935–942, <https://doi.org/10.1145/1273496.1273614>, 2007.

691 Virkkala, A.-M., Aalto, J., Rogers, B. M., Tagesson, T., Treat, C. C., Natali, S. M., Watts, J. D.,
692 Potter, S., Lehtonen, A., Mauritz, M., Schuur, E. A. G., Kochendorfer, J., Zona, D., Oechel, W.,
693 Kobayashi, H., Humphreys, E., Goeckede, M., Iwata, H., Lafleur, P. M., Euskirchen, E. S., Bokhorst,
694 S., Marushchak, M., Martikainen, P. J., Elberling, B., Voigt, C., Biasi, C., Sonnentag, O., Parmentier,
695 F.-J. W., Ueyama, M., Celis, G., St.Louis, V. L., Emmerton, C. A., Peichl, M., Chi, J., Järveoja, J.,
696 Nilsson, M. B., Oberbauer, S. F., Torn, M. S., Park, S.-J., Dolman, H., Mammarella, I., Chae, N.,
697 Poyatos, R., López-Blanco, E., Christensen, T. R., Kwon, M. J., Sachs, T., Holl, D., and Luoto, M.:
698 Statistical upscaling of ecosystem CO₂ fluxes across the terrestrial tundra and boreal domain:
699 Regional patterns and uncertainties, *Global Change Biology*, 27, 4040–4059,
700 <https://doi.org/10.1111/gcb.15659>, 2021.

701 Walther, S., Besnard, S., Nelson, J. A., El-Madany, T. S., Migliavacca, M., Weber, U., Ermida, S. L.,
702 Brümmer, C., Schrader, F., Prokushkin, A. S., Panov, A. V., and Jung, M.: Technical note: A view
703 from space on global flux towers by MODIS and Landsat: The FluxnetEO dataset, *Biogeosciences*
704 *Discussions*, 1–40, <https://doi.org/10.5194/bg-2021-314>, 2021.

705 Wu, Z., Dijkstra, P., Koch, G. W., Peñuelas, J., and Hungate, B. A.: Responses of terrestrial
706 ecosystems to temperature and precipitation change: a meta-analysis of experimental manipulation,
707 *17*, 927–942, <https://doi.org/10.1111/j.1365-2486.2010.02302.x>, 2011.

708 Yan, J., Zhang, Y., Yu, G., Zhou, G., Zhang, L., Li, K., Tan, Z., and Sha, L.: Seasonal and inter-
709 annual variations in net ecosystem exchange of two old-growth forests in southern China, *Agricultural*
710 *and Forest Meteorology*, 182–183, 257–265, <https://doi.org/10.1016/j.agrformet.2013.03.002>, 2013.

711 Zeng, J., Matsunaga, T., Tan, Z.-H., Saigusa, N., Shirai, T., Tang, Y., Peng, S., and Fukuda, Y.:
712 Global terrestrial carbon fluxes of 1999–2019 estimated by upscaling eddy covariance data with a
713 random forest, *7*, <https://doi.org/10.1038/s41597-020-00653-5>, 2020.

714 Zhang, C., Brodylo, D., Sirianni, M. J., Li, T., Comas, X., Douglas, T. A., and Starr, G.: Mapping
715 CO₂ fluxes of cypress swamp and marshes in the Greater Everglades using eddy covariance
716 measurements and Landsat data, *Remote Sensing of Environment*, 262,
717 <https://doi.org/10.1016/j.rse.2021.112523>, 2021.

718 Zhou, Y., Li, X., Gao, Y., He, M., Wang, M., Wang, Y., Zhao, L., and Li, Y.: Carbon fluxes response
719 of an artificial sand-binding vegetation system to rainfall variation during the growing season in the
720 Tengger Desert, *Journal of Environmental Management*, 266,
721 <https://doi.org/10.1016/j.jenvman.2020.110556>, 2020.

722 Zhu, S., Clement, R., McCalmont, J., Davies, C. A., and Hill, T.: Stable gap-filling for longer eddy
723 covariance data gaps: A globally validated machine-learning approach for carbon dioxide, water, and
724 energy fluxes, *Agricultural and Forest Meteorology*, 314, 108777,
725 <https://doi.org/10.1016/j.agrformet.2021.108777>, 2022.

726